View metadata, citation and similar papers at core.ac.uk

brought to you by CORE

provided by Purdue E-Pubs

Purdue University
Purdue e-Pubs

Department of Earth, Atmospheric, and Planetary Sciences Faculty Publications

Department of Earth, Atmospheric, and Planetary Sciences

6-21-2009

Orbitally forced climate changes in the Tasman sector during the Middle Eocene

Jeroen Warnaar
Utrecht University, Budapestlaan 4, 3584 CD Utrecht, The Netherlands

Peter K. Bijl
Utrecht University, Budapestlaan 4, 3584 CD Utrecht, The Netherlands

Matthew Huber
Purdue, huber@purdue.edu

Lisa Sloan
Univ. of California

Henk Brinkhuis
Utrecht University, Budapestlaan 4, 3584 CD Utrecht, The Netherlands

See next page for additional authors

Follow this and additional works at: http://docs.lib.purdue.edu/easpubs

Repository Citation

Warnaar, Jeroen; Bijl, Peter K.; Huber, Matthew; Sloan, Lisa; Brinkhuis, Henk; Röhl, Ursula; Sriver, Ryan; and Visscher, Henk, "Orbitally forced climate changes in the Tasman sector during the Middle Eocene" (2009). *Department of Earth, Atmospheric, and Planetary Sciences Faculty Publications.* Paper 88.
http://dx.doi.org/http://dx.doi.org/10.1016/j.palaeo.2009.06.023

This document has been made available through Purdue e-Pubs, a service of the Purdue University Libraries. Please contact epubs@purdue.edu for additional information.

Authors
Jeroen Warnaar, Peter K. Bijl, Matthew Huber, Lisa Sloan, Henk Brinkhuis, Ursula Röhl, Ryan Sriver, and Henk Visscher

This article is available at Purdue e-Pubs: http://docs.lib.purdue.edu/easpubs/88

Palaeogeography, Palaeoclimatology, Palaeoecology 280 (2009) 361–370

Contents lists available at ScienceDirect

Palaeogeography, Palaeoclimatology, Palaeoecology

journal homepage: www.elsevier.com/locate/palaeo

Orbitally forced climate changes in the Tasman sector during the Middle Eocene

Jeroen Warnaar [a], Peter K. Bijl [a,*], Matthew Huber [b], Lisa Sloan [c], Henk Brinkhuis [a], Ursula Röhl [d], Ryan Sriver [b,1], Henk Visscher [a]

[a] Laboratory of Palaeobotany and Palynology, Utrecht University, Budapestlaan 4, 3584 CD Utrecht, The Netherlands
[b] Earth & Atmospheric Sciences, 1397 Civil Engineering Bldg., Purdue University, West Lafayette, IN 47907-1397, USA
[c] Earth & Planetary Sciences Department, Earth & Marine Sciences, University of California, Santa Cruz, CA 95064, USA
[d] MARUM — Center for Marine Environmental Sciences, University of Bremen, Leobener Strasse, 28359 Bremen, Germany

ARTICLE INFO

Article history:
Received 28 May 2008
Received in revised form 9 June 2009
Accepted 12 June 2009
Available online 21 June 2009

Keywords:
Southern Ocean
Middle Eocene
Orbital forcing
Model-data comparison
Organic-walled dinoflagellate cysts
General circulation model

ABSTRACT

The influence of orbital precession on early Paleogene climate and ocean circulation patterns in the southeast Pacific region is investigated by combining environmental analyses of cyclic Middle Eocene sediments and palynomorph records recovered from ODP Hole 1172A on the East Tasman Plateau with climate model simulations. Integration of results indicates that in the marine realm, direct effects of precessional forcing are not pronounced, although increased precipitation/runoff could have enhanced dinoflagellate cyst production. On the southeast Australian continent, the most pronounced effects of precessional forcing were fluctuations in summer precipitation and temperature on the Antarctic Margin. These fluctuations resulted in vegetational changes, most notably in the distribution of *Nothofagus* (subgenus *Brassospora*). The climate model results suggest significant fluctuations in sea ice in the Ross Sea, notably during Austral summers. This is consistent with the influx of Antarctic heterotrophic dinoflagellates in the early part of the studied record. The data demonstrate a strong precessionally driven climate variability and thus support the concept that precessional forcing could have played a role in early Antarctic glaciation via changes in runoff and/or precipitation.

© 2009 Elsevier B.V. All rights reserved.

1. Introduction

Apart from the tectonic and related oceanographic variables, model studies indicate that orbital cyclicity should also be regarded as a significant forcing factor influencing Paleogene climatic conditions on Antarctica (DeConto and Pollard, 2003a; DeConto et al., 2007). Röhl et al. (2004) documented the presence of cyclic sediments of Eocene age offshore East Tasmania (Ocean Drilling Program Leg (ODP) 189, Holes 1172A and D). In the recorded cyclic patterns, represented by fluctuations in sediment input of marine and continental origin, a full power spectrum of orbital frequencies is apparent, where precession is the most prominent component (Röhl et al., 2004). This is surprising because obliquity is normally considered to play a dominant role in high latitude climate variability, whereas precession is usually considered important in the tropics (Ruddiman, 2001). We examine this issue more in depth in this paper and use climate models to demonstrate that physical processes could explain the precession-dominated cyclicity in these high latitude proxy records.

In order to assess the role of precession on climatic conditions in the southwest Pacific region and on surface circulation patterns in the Southern Ocean, an environmental reconstruction of the Middle Eocene palynomorph record from the cyclic sediments of ODP Hole 1172A is made. Palynomorphs are abundant and well preserved in the sediments. Assemblages contain both marine dinoflagellate cysts (dinocysts) and land-derived pollen and spores (sporomorphs) enabling detailed correlation of coeval marine and continental environmental signals. Considering Paleogene surface currents (Huber et al., 2004) and wind patterns (Warnaar, 2006) over the East Tasman Plateau, the analysed microfossils (both wind blown and water transported) are at least in part derived from the Antarctic region, in addition to the local Tasman communities. The paleoenvironmental reconstruction is compared to an experiment carried out with an atmospheric general circulation model (GCM) coupled to a 'slab' ocean. The GCM experiment, with Eocene boundary conditions, is set up to simulate the effect of precession Two different model runs are carried out with identical setup, except that each run has a different solar insolation pattern representing an opposite precessional extremes, with obliquity and eccentricity changed accordingly (see Sloan and Huber, 2001, for details). The model output and the palynological results are subsequently integrated into a detailed

* Corresponding author. Tel.: +31 30 253 9318.
E-mail addresses: p.k.bijl@uu.nl (P.K. Bijl), huberm@purdue.edu (M. Huber), lsloan@es.ucsc.edu (L. Sloan), uroehl@marum.de (U. Röhl).
[1] Now at: Department of Meteorology and Earth and Environmental Systems Institute, Pennsylvania State University, University Park, PA 16802, USA.

0031-0182/$ – see front matter © 2009 Elsevier B.V. All rights reserved.
doi:10.1016/j.palaeo.2009.06.023

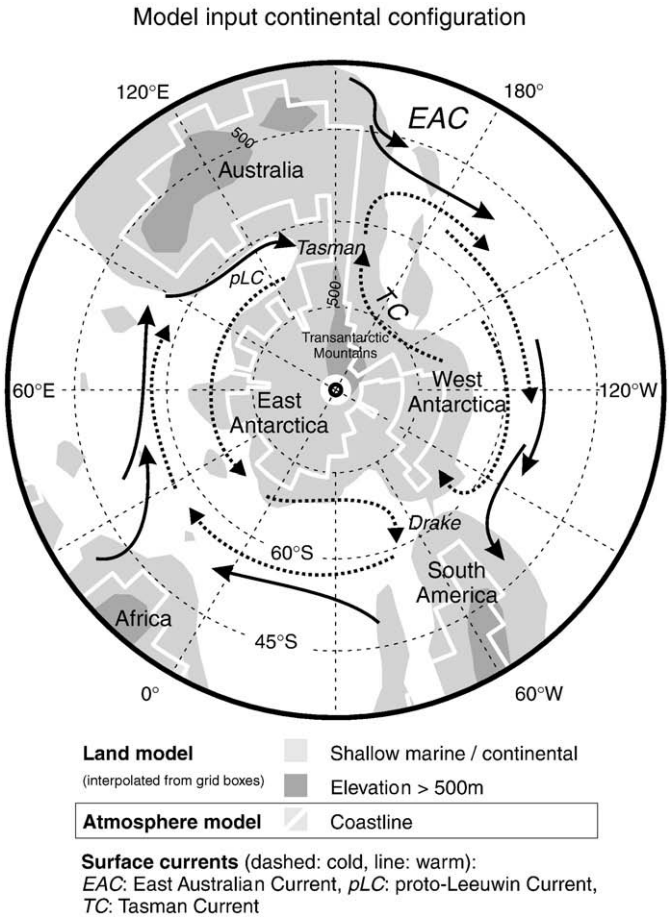

Fig. 1. Model input continental configuration (land model: shaded; atmosphere model lines) and derived ocean surface circulation patterns.

paleo-environmental reconstruction. Implications for the early Paleocene climate history of Antarctica and the southwest Pacific are discussed (Figs. 1 and 2).

2. Materials and methods

2.1. Sedimentary data materials and methods

Material was selected from Ocean Drilling Program Leg 189, Hole 1172A, which was drilled on the East Tasman Plateau (ETP), at 43°58' S, 149°56' E, at 2622 m water depth (Exon et al., 2001). Eocene sediments are nannofossil-bearing, diatomaceous, silty claystones, deposited under shallow marine (~100–200 m water depth) conditions (Exon et al., 2001, 2004). The Cascade Seamount volcano, East of the Site on the ETP, was active throughout the Eocene (Quilty, 1997). As a result of further opening and notably deepening of the Tasmanian Gateway, the siliciclastic sediments grade into glauconitic sandstones in the latest Eocene which, in turn, are overlain by Oligocene and younger calcareous ooze (Royer and Rollet, 1997; Exon et al., 2001).

With X-ray fluorescence (XRF) measurements, Röhl et al. (2004) identified cyclic patterns in the Middle to Late Eocene sediments of Site 1172, Holes A and D. The patterns represent alternations in the concentration of calcium, reflecting $CaCO_3$ of marine origin; and iron, reflecting continental clays and volcanic material. Because the iron record displays considerably more "noise" due to the ferrous nature of the volcanic material, the calcium record is used. Although recovery was good for a single hole, recovery gaps and hiatuses at core breaks occur. Despite incompleteness of the record, Röhl et al. (2004) could attribute fluctuations in calcium concentration in the 0.4–0.5 m range to orbital precession because (**1**) the number of cycles, and the time span they represent, corresponds with the duration of the magnetic intervals (Fuller and Touchard, 2004), (**2**) the full power spectrum (i.e., all different precession, obliquity and eccentricity frequencies) could be articulated, in which the precession bands (19–23 kyr) could be distinguished, and (**3**) the cycles generally show double peaks, of which one is more pronounced, a feature that is typical for precession cyclicity (19–23 kyr) modulated by eccentricity.

The interval with the most distinct cyclic pattern is selected (Röhl et al., 2004), namely Core 43X, Sections 1–4 (between 394 and 398 meters below sea floor (mbsf)); magnetic interval C18n.1n; age ~38.5 Ma (Gradstein et al., 2004). The interval covers 10 $CaCO_3$ cycles, that are numbered 1*a*, 1*b* and 2–9 and includes two distinct volcaniclastic sediment layers (at 394.5 and 395.2 mbsf). Cycles 1*a* and 1*b* represent in effect a single cycle, cut in two by a volcaniclastic sediment layer (Ash 1; see Fig. 3). Between 394.3 and 396 mbsf the record is slightly expanded (by a factor of 1.3) due to increased terrestrial and/or volcanic sediment input. Sedimentation rate is ~2 cm/kyr, and ~2.5 cm/kyr in the expanded part (Robert, 2004; Röhl et al., 2004). With loss on ignition (LOI; Heiri et al., 2001) the $CaCO_3$ content of the sediments, taken from the working half of the core, was determined independently, and correlated to the XRF data set, which was measured on the archive half (see Fig. 3). Because the volcaniclastic sediment layers probably reflect instantaneous volcanic events, they were taken out of the record (after correlation of both core-halves). Eighty-six palynological samples are taken at 5 cm intervals.

Palynological processing was performed following the standardized quantitative methods used at the Laboratory of Palaeobotany and Palynology, Utrecht University (Brinkhuis et al., 2003). Briefly, this involved processing using ~20% HCl and ~30% HF, and ultrasound separation. No bleaching and heavy liquid separation was applied. 12 µm nylon mesh was used for sieving of the residues. With a micropipette a fixed amount (20.0 µl of 1.0 ml) of material was transferred to a slide, allowing quantitative dinocyst estimations (cysts/g sediment). Where possible, over 200 dinocysts were counted per sample and identified to the species level. Some slides contained fewer dinocysts, and there the entire slide was counted. Four samples contained less than 100 dinocysts, with a minimum of 78. Spores of *Lycopodium* were added prior to processing and counted in the slides to detect significant loss of palynomorphs. Nomenclature and taxonomy, unless stated otherwise, was based on (Brinkhuis et al., 2003; Williams et al., 2004; Fensome and Williams, 2004). Samples and slides are stored in the collection of the Laboratory of Palaeobotany and Palynology, Utrecht University, The Netherlands. Principal component analysis was used to analyze the data (Fig. 4).

2.2. General Circulation Model setup

2.2.1. General Circulation Model

This study uses the general circulation model (GCM) GENESIS 2 (Sloan and Huber, 2001). It is an atmosphere GCM coupled to a land model, a sea ice model and a 50 m deep mixed layer slab ocean model. The land model has a 2° by 2° resolution latitude by longitude grid size and the atmosphere model has a ~3.75° by 3.75° resolution latitude by longitude grid size. We have analyzed the effects of precession variability extensively utilizing these simulations previously and validated the model prediction in several regions (Huber and Sloan, 2001). For further model setup and sensitivity reports see (Sloan and Morrill, 1998; Huber and Sloan, 2000; Huber and Sloan, 2001). The boundary conditions of the GCM are set to represent the Middle Eocene situation (Sloan and Huber, 2001). Crucial aspects, such as greenhouse gases and the geographical setup are discussed below.

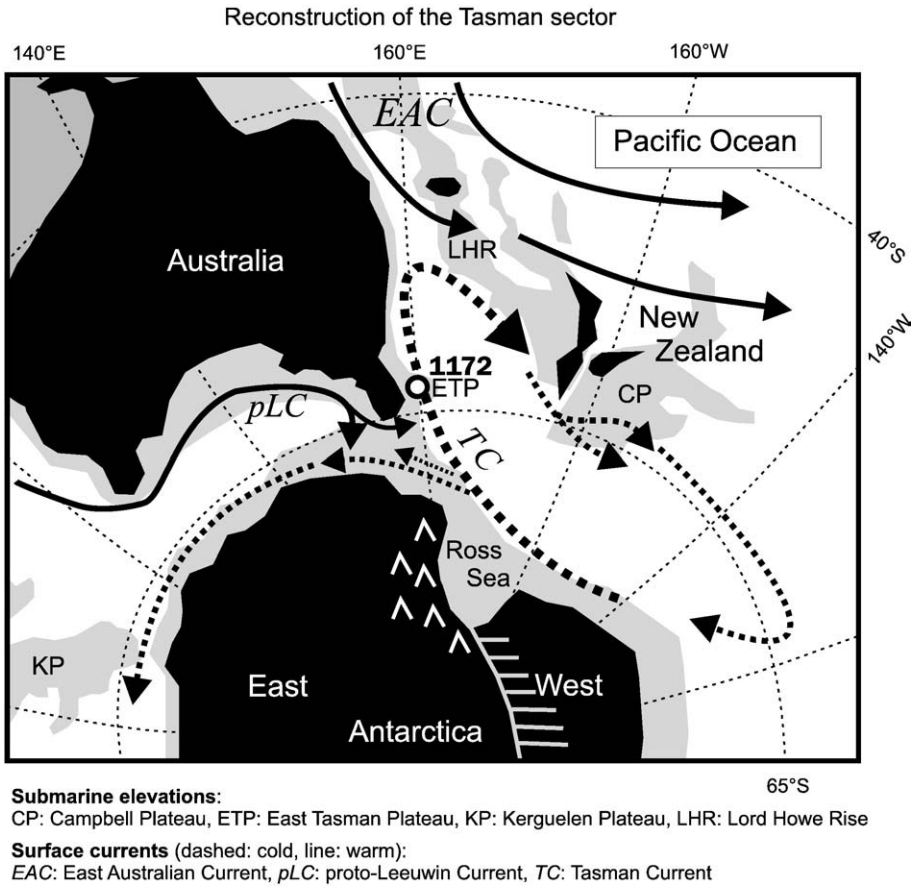

Fig. 2. Reconstruction of the Tasman Sector: Middle Eocene (~39 Ma): Tectonic map and ocean surface currents. Tectonic configuration map (B) based on (Norvick and Smith, 2001; Hay et al., 1999; http://www.odsn.de/odsn/services/paleomap/paleomap.html; Langford et al., 1995). Surface ocean circulation patterns based on (Huber and Sloan, 2000; Huber and Sloan, 2001; Huber et al., 2004).

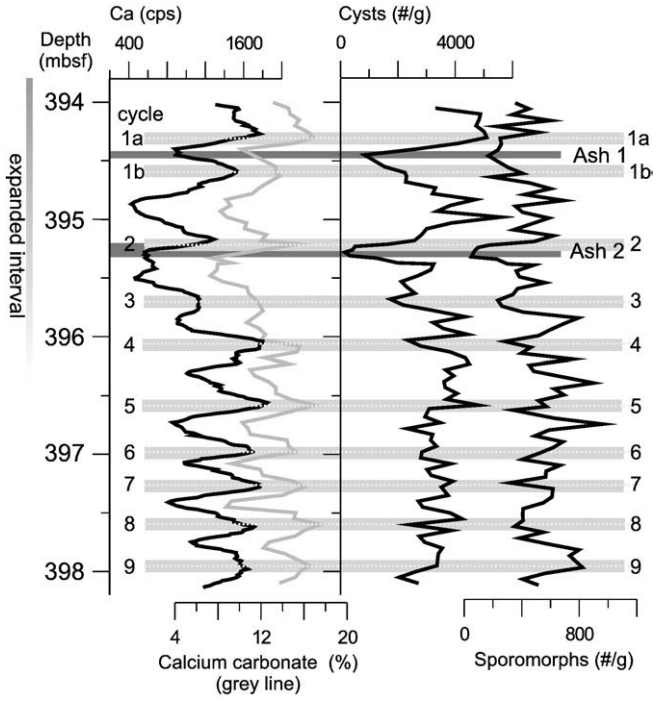

Fig. 3. Sedimentary data (1): ODP Hole 1172A, 394–398 mbsf. Left: Calcium content (counts per second, cps) and $CaCO_3$ content (%). The shaded bands, Ash 1 and Ash 2 indicate layers of volcaniclastic material. Right: Absolute values of dinocysts (cysts/g sediment) and sporomorphs (pollen and spores/g sediment).

2.2.2. Greenhouse gases

The concentration of atmospheric CO_2 is believed to have followed a declining, though fluctuating, trend since the Middle Eocene Climatic Optimum (MECO; Pagani et al., 2005). From values well above 1000 ppmv, CO_2 levels declined to present-day values in the Oligocene (Roth-Nebelsick et al., 2004; Pagani et al., 2005). Conservative evaluation of proxy CO_2 estimates for the late Middle Eocene (~39 Ma) gives a range between 500 and 700 ppmv (see references in Sloan and Rea, 1995; Pearson and Palmer, 2000; Kürschner et al., 2001; Pagani et al., 2005). Hence, in the model, CO_2 concentration is set at double pre-industrial values (560 ppmv). Other greenhouse gas concentrations (CH_4 and N_2O), for which no proxy data are available, are kept at pre-industrial levels.

2.2.3. Precession cases Pr1 and Pr2 model runs

Two model runs are performed, the Pr1 and Pr2 case. In the Pr1 case the Earth is closest to the Sun (perihelion) during Southern Hemisphere (Austral) winter and farthest away from the Sun (aphelion) during Austral summer. This generates reduced Austral seasonality, with milder winters (June–July–August; JJA) and cooler summers (December–January–February; DJF). The Pr2 case generates the reversed situation, where Austral seasonality is amplified, with warmer Austral (perihelion) summers and cooler Austral (aphelion) winters. Pr1 and Pr2 are each run for four full years (48 months), after spin up. While changing the precession parameter in the orbital insolation between the Pr1 and Pr2 case (by half a precession cycle, or 11.5 kyr further), obliquity and eccentricity parameters are changed accordingly (Sloan and Huber, 2001). A Student's *t*-test (two tailed, with a 95% confidence interval) is used

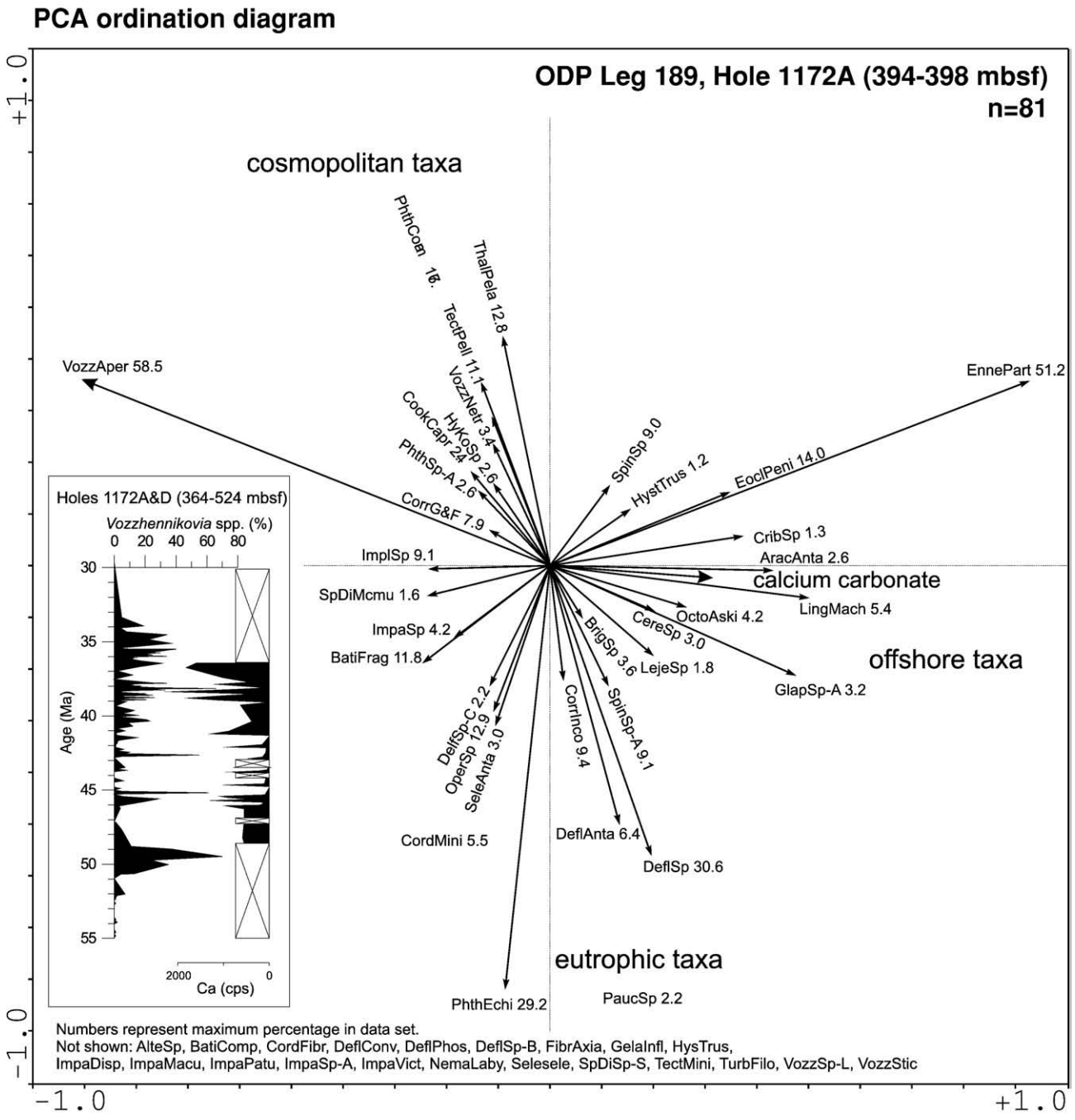

Fig. 4. Principal component analysis (PCA) is used to analyse the dinocyst data set. Determined are the (two) best explanatory variables for the composition of the dinocyst assemblages. Canoco for Windows (V.4.02) and Canodraw (V.3.1) are utilized. The percentages of the taxa per sample are used, and not absolute numbers per gram, to avoid over-representation of samples rich in dinocysts (see Fig. 3). Results are shown in the ordination diagram above. All taxa are included in the calculation, but taxa with a maximum occurrence of 1% or less, are not shown as arrows. The first axis explains 53.7% of the variance within the data set, while the second axis explains 18.3%. Dinocyst taxa are coded using the first four letters of the genus name followed by the first four letters of the species name (or simply '-Sp') (e.g., DeflAnta' = *Deflandrea antarctica*). The exception is that 'SpDi-' = *Spinidinium*, (because 'Spin-' = *Spiniferites*).

to determine if differences between the Pr1 and Pr2 output are statistically significant. The null hypothesis (H_0) of the test assumes that the averages (taken over 4 years) of each Pr-case are of the same population. All the described features in this paper are significant at >95% confidence level.

We will now show how the palynological assemblage in the sediment is related to the precession-forced $CaCO_3$ cycles, and compare these results with the modeled surface temperature, pressure and precipitation variation over the two extreme precession cases.

3. Results

3.1. Sedimentary data

Dinocyst absolute abundance is represented by the total number of cysts per gram of sediment (Fig. 3). In cycles 1–5 (i.e., the expanded part of the interval), cyst abundance shows an inverse correspondence with the $CaCO_3$ cycles. However, between cycle tops 6 and 9, no such, or other relationship can be discerned. Sporomorph absolute

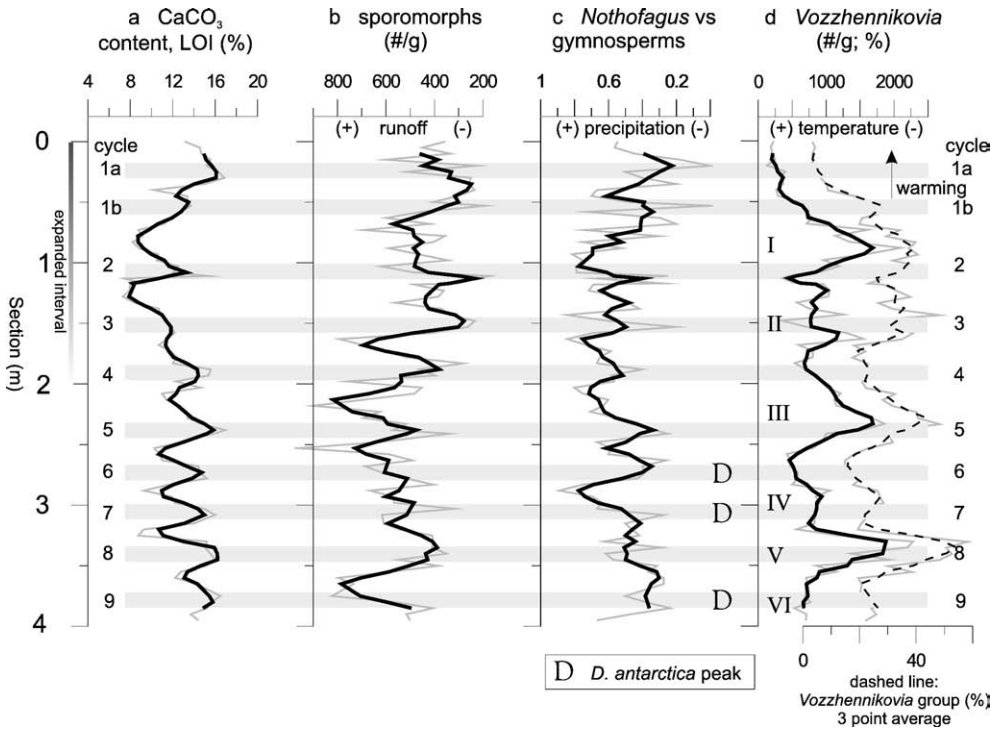

Fig. 5. Sedimentary data (2): ODP Hole 1172A (394–398 mbsf shown as 1–4 m; volcanic layers are not shown). $CaCO_3$ content (a) compared with sporomorphs (pollen and spores/g sediment; b); *Nothofagus* pollen versus gymnosperm pollen (i.e., N/N + G; c) and *Vozzhennikovia apertura* (cysts/g sediment and percentage of all dinocysts; d). Grey thin lines indicate the measured/calculated values. Thick black lines indicate three-point running average smoothing.

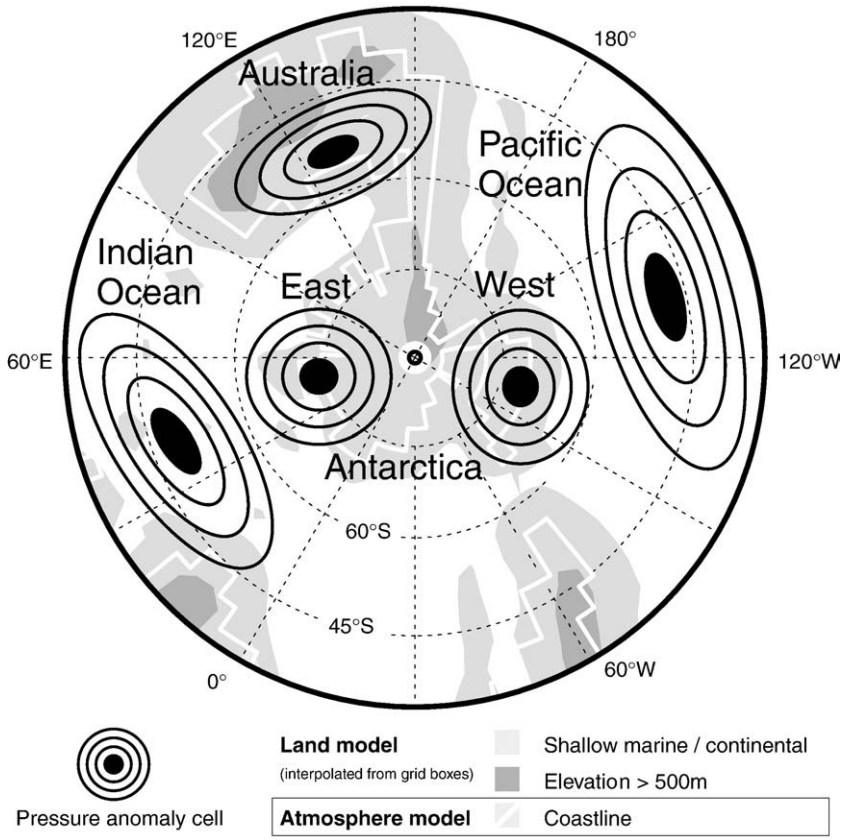

Fig. 6. GCM results: Geographical distribution of quasi-stable atmospheric pressure anomaly cells (ground level).

abundance also has an inverse relationship with the $CaCO_3$ cycles (Fig. 3). Throughout the record the sporomorphs have distinct peak occurrences at low $CaCO_3$ values. In the lower part of the interval however (cycles 7–9), this relationship is less evident.

Considerable fluctuations are recorded within the dinocyst assemblages throughout the interval. Most variation seems unrelated to precession cycles, and is therefore not considered here. However, *Vozzhennikovia apertura* displays a distinct cyclic pattern, both in total (cysts/gr) and relative abundance. The cycles, some are more pronounced than others, are numbered I to VI (Fig. 5). Distance between cycles I and IV is ~0.8 m, and the distance between the lowermost three cycles (IV–VI) is ~0.4 m. The lower frequency cycles do not seem to be related to the $CaCO_3$ cycles, while the maxima of IV–VI co-occur with the calcium maxima of cycles 7–9. Interestingly, three $CaCO_3$ cycles in the lower part of the interval (6, 7 and 9) are also in phase with three distinct peak abundances of *Deflandrea antarctica* (Fig. 5). Three subgroups characterize the sporomorph assemblage: saccate conifer pollen (mainly *Podocarpus*), *Nothofagus* (mainly the pollen morphotype corresponding to the subgenus *Brassospora*), and fern spores. Other groups (i.e., non-*Nothofagus* angiosperm pollen and conifer pollen representing *Araucariaceae*) are represented by numbers that are too low to draw conclusions from. Closer inspection reveals that the inverse relationship between sporomorphs and the $CaCO_3$ cycles is mainly caused by fluctuations of *Nothofagus* pollen (Fig. 5). In the next section we explore potential physical mechanisms by which these periodicities may have entered the record by comparing with the climate model output.

3.2. GCM results

Oscillating climate systems can often be characterized as spatial variations in atmospheric pressure (e.g., the El Niño Southern Oscillation, the North Atlantic Oscillation and the Antarctic Oscillation). The differences between the two modelled precession cases (Pr1 and Pr2) are in the order of ±2.5 hPa, with extremes exceeding 6 hPa (Fig. 6). The centres of action indicated from the pressure anomalies can be represented in a simplified fashion by five anomaly cells (Fig. 6). Two cells are situated above West and East Antarctica, respectively. The cell above East Antarctica extends above the southeastern part of the Indian Ocean. A third cell is formed above Australia. The two remaining cells are located at about 40°S above the South Pacific and the southwestern Indian Ocean. Both Antarctic cells have a higher pressure in the Pr2 case during the Austral summers and winters (Table 1; Figs. 6 and 7). In contrast to the two seasonally 'stable' cells above Antarctica, the oceanic and Australian cells have a strong seasonal component. For example, the anomaly cell above the southwestern Indian Ocean is only present during Austral Winter (JJA; June–July–August), where pressure is higher in the Pr1 situation (Table 1).

Climatic features, such as temperature, wind strength and precipitation follow the same pattern as observed for pressure (Table 1; Fig. 6). For example, areas of decreased pressure are characterized by increased wind strength and precipitation, while increased pressure causes the reverse situation. Lower surface temperatures normally co-occur with higher sea-level pressure (and *vice versa*). Upper ocean circulation patterns and current strength are directly related to the surface wind strength and direction (Huber and Nof, 2006), unless wind–ocean interaction is prevented by sea ice. The extent of sea ice is principally restricted to the Ross Sea and seems mainly determined by the Austral winter surface temperature (which is lower in Pr1).

4. Discussion

4.1. Integration of field data and GCM results

Varying amounts of terrestrial sedimentary input in shallow marine sediments are generally caused by either fluctuations in sea-

Table 1
Summary of GCM results. Relative differences between Pr1 and Pr2 cases. Differences between brackets are small, but still significant (Student's *t*-test, see Materials and methods).

	Annual average		Summer DJF		Winter JJA	
Model case	Pr1	Pr2	Pr1	Pr2	Pr1	Pr2
Seasonality SH average	Reduced	Enhanced	Milder	Warmer	Milder	Colder
Sea level pressure						
Tasmania/SE Australia	–	–	Lower	Higher	Higher	Lower
Ross sea	–	–	–	–	(Higher)	(Lower)
West Antarctica	Lower	Higher	Lower	Higher	Lower	Higher
East Antarctica	Lower	Higher	(Lower)	(Higher)	Lower	Higher
South Pacific Ocean (45°)	–	–	Higher	Lower	Lower	Higher
South Indian Ocean (45°)	Higher	Lower	–	–	Higher	Lower
Surface temperature						
Tasmania/SE Australia	–	–	Warmer	Cooler	–	–
Ross sea	Cooler	Warmer	–	–	Cooler	Warmer
West Antarctica	Warmer	Cooler	Mixed	Mixed	Warmer	Cooler
East Antarctica	Warmer	Cooler	Warmer	Cooler	Warmer	Cooler
South Pacific Ocean (45°)	–	–	–	–	(Warmer)	(Cooler)
South Indian Ocean (45°)	–	–	(Warmer)	(Cooler)	(Warmer)	(Cooler)
Surface wind strength						
Tasmania/SE Australia	–	–	–	–	–	–
Ross sea	–	–	–	–	Lower	Higher
West Antarctica	–	–	(lower)	(higher)	Higher	Lower
East Antarctica	–	–	Higher	Lower	–	
South Pacific Ocean (45°)	–	–	Lower	Higher	Higher	Lower
South Indian Ocean (45°)	Lower	Higher	–	–	Lower	Higher
Precipitation (rainfall)						
Tasmania/SE Australia	–	–	Higher	Lower	(lower)	(higher)
Ross sea	–	–	Lower	Higher	–	–
West Antarctica	–	–	Lower	Higher	Higher	Lower
East Antarctica	Higher	Lower	–	–	Higher	Lower
South Pacific Ocean (45°)	–	–	Lower	Higher	Higher	Lower
South Indian Ocean (45°)	–	–	–	–	(Lower)	(Higher)

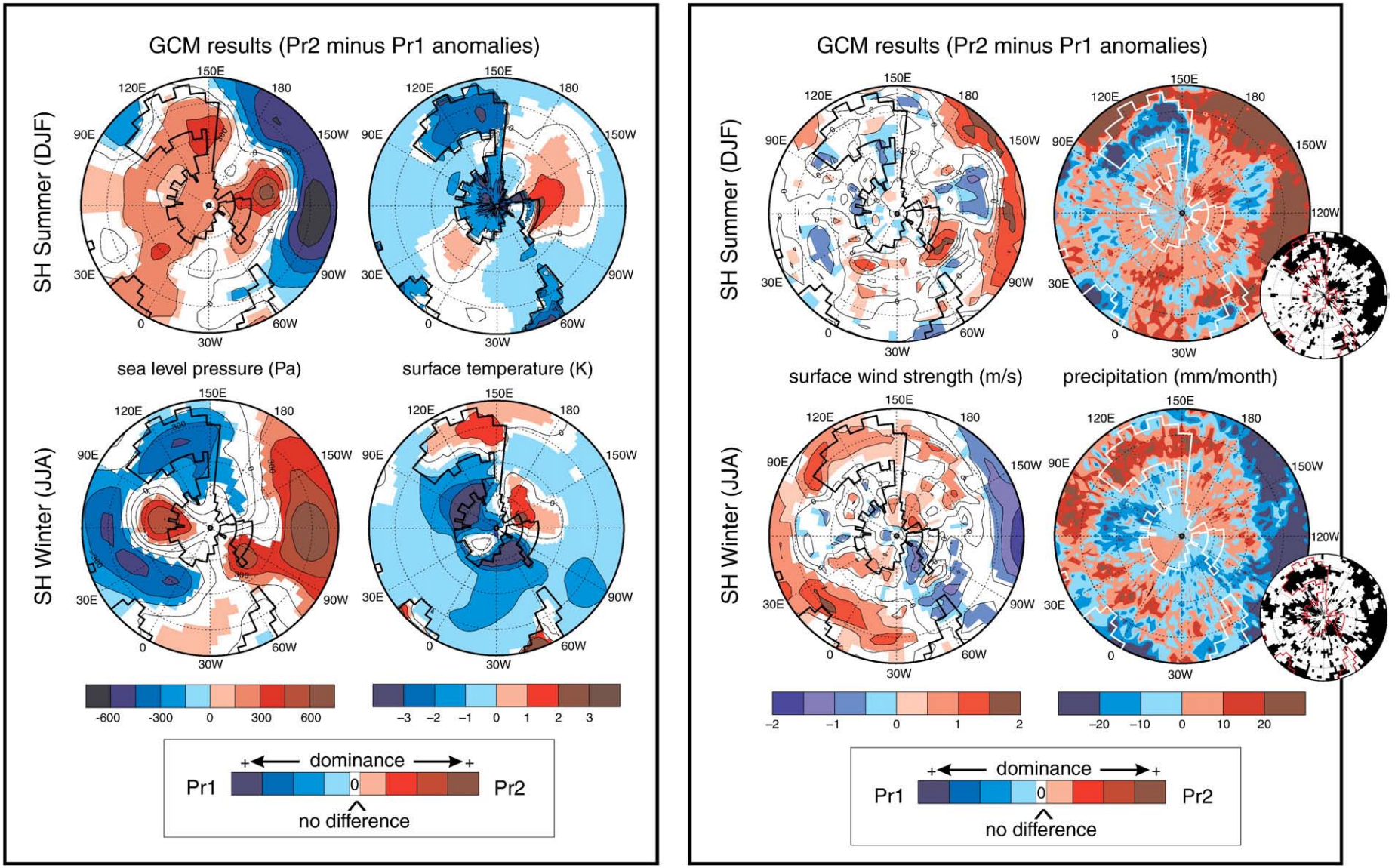

Fig. 7. GCM results, showing the differences in sea level pressure (Pa), surface temperature (K), surface wind strength (m/s) and precipitation (mm/month) between model runs Pr1 and Pr2. Absolute values of Pr1 results are subtracted from the results of Pr2. Red areas indicate higher values during Pr2, and blue areas higher values during Pr1. White areas (inlays for precipitation results) indicate areas where no significant difference is observed between Pr1 and Pr2 (see Materials and methods). Superimposed are the continental outlines of the atmosphere model (thick lines).

level or fluctuations in aridity/precipitation on an adjacent continent. Röhl et al. (2004) attributed large-scale cyclic patterns observed at Site 1172 (Holes A and D) to third-order sea-level changes (in the order of millions of years). It has been postulated that during the Eocene small ice sheets already existed in the elevated areas of Antarctica (e.g., Kerr and Huybrechts, 1999; Zachos et al., 2001). However, the high frequency (tens of thousands of years) fluctuations of these small Antarctic ice sheets (driven by orbital forcing) are thought to have caused sea-level changes in the order of only a few meters (DeConto and Pollard, 2003a; DeConto et al., 2007). Fluctuations on this scale would probably have no apparent effect on sedimentation on the East Tasman Plateau. This argument is confirmed here. High resolution sedimentary cycles had been identified in a section from New Zealand (Burgess et al., 2008). This record shows no evidence for sea level fluctuations that can be related to waxing and waning of ice sheets, however they do note substantial climate variability on precessional time scales. Low resolution dinocyst assemblage analyses at Site 1172 have previously been described to show prominent variability related to sea level fluctuations (Röhl et al., 2004). By studying the dinocyst assemblages on precessional scale resolution, we identify an additional short term dinocyst assemblage variability. The GCM output indicated distinct fluctuations in precipitation (see Fig. 7; Table 1) that may have caused the cyclic pattern through fluctuating runoff and sediment input. Hence, concluding from the above, we attribute the recognized precessional cyclicity in the sedimentary record to changes in precipitation/runoff, rather than sea level change.

The relationship between the $CaCO_3$ cycles and the palynomorph record shows a break at and below cycle 6. In cycles 1–6, the inverse relationship between absolute numbers of palynomorphs and the $CaCO_3$ content can be explained by fluctuating terrestrial sediment supply (see above). Increased precipitation and accompanied runoff occurs in the Austral summer Pr2 (see Figs. 7 and 8), causing an increased transport of terrigenous material, including sporomorphs, from the Antarctic continent, into the Southwest Pacific. These are then transported northward to the East Tasman Plateau. Also, the modelled higher temperatures that coincides with increased precipitation (i.e., Pr2 Austral summer; Fig. 8) would cause more favourable growing conditions for vegetation along the Antarctic coastline, resulting in enhanced sporomorph production.

In addition, the elevated nutrient input associated with increased runoff is likely to boost the growth of many algal groups, such as dinoflagellates (e.g., Wasmund et al., 1999; Reichart and Brinkhuis, 2003). This could explain why the dinocysts and sporomorphs follow the same pattern in cycles 1–5 (see Fig. 3). Furthermore, increased sedimentation and microbial breakdown of organic material generates CO_2, which may result in a slight acidification of the water column causing partial dissolution of the calcareous fraction.

Trees and shrubs of *Nothofagus (Brassospora)* are characteristic for highland temperate rainforests (Sluiter et al., 1995; Mildenhall et al., 2004), where changes in temperature and precipitation have the most pronounced effect. Hence, the conditions that are favourable for *Nothofagus (Brassospora)* occur during Pr2 (Figs. 5 and 8). In the Pr1 case, growing conditions of *Nothofagus* populations in highland areas would be significantly disturbed, while effects on other groups like *Podocarpus,* ferns, growing in coastal areas (Sluiter et al., 1995) are less severe (Fig. 5).

Vozzhennikovia apertura appears to be associated with the cold circum-Antarctic shallow shelf areas (Wilson, 1967; Hannah, 1997;

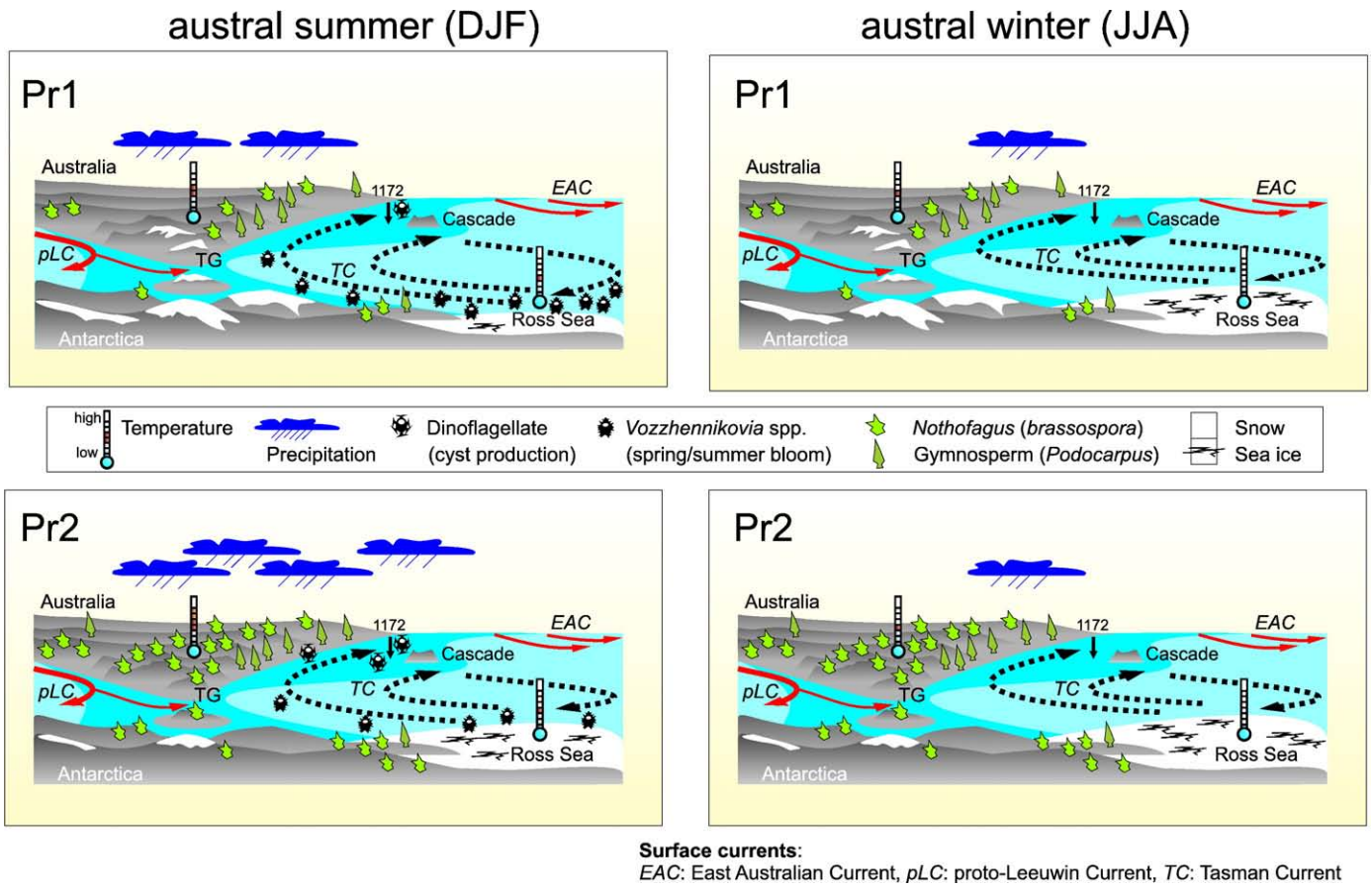

Fig. 8. Simplified reconstruction scheme indicating differences in precipitation, surface temperature, snow cover, sea ice, vegetation cover and dinoflagellate distributions of Pr1 and Pr2 austral summer and winter cases.

Mohr, 1990; Macphail and Truswell, 2004). The conjectured cold Tasman Current (Huber et al., 2004), flowing from the Ross Sea (see Fig. 1 and 2), probably controlled the occurrence of this taxon on the East Tasman Plateau (Warnaar, 2006). While a straightforward (inverse) relationship with the $CaCO_3$ cycles is not detected, principal component analysis (PCA) of the data set (thus disregarding the time-series cyclic aspect) shows that the $CaCO_3$ concentration strongly correlates inversely with the percentage of *V. apertura* (Fig. 5). PCA analysis of the lower resolution data set that covers most of the Middle and Late Eocene gives similar results (Röhl et al., 2004). Hence it seems that high $CaCO_3$ concentrations, predominantly determined by the amount of nannofossils, portray warmer and/or more offshore (likely more oligotrophic) conditions, whereas high concentrations of *V. apertura* reflect the reversed situation. The overall wavelength of the *V. apertura* cycles in our record is ~0.8 m, much longer than the precession-scale calcium counts. Tentatively, the *V. apertura* cyclicity is obliquity (41 kyr) paced, an important orbital frequency at high latitudes. However, comparing the 5.5 *V. apertura* cycles to the 9 precession cycles in the calcium record indicates a periodicity of 35 kyrs (9 cycles of 21 kyrs is 189 kyrs, divided by 5.5 *V. apertura* cycles), which is shorter than the obliquity periodicity. Hence, on a longer periodicity than precession, fluctuations in the abundance of *V. apertura* can not conclusively be attributed to obliquity. From 0.5 m upward in the interval studied, *V. apertura* gradually diminishes, to be replaced by cosmopolitan taxa, which could indicate a weakening of the Tasman Current and warming. In contrast to cycles 1–6, in cycles 7–9 (the lower part of the studied interval) the *V. apertura* cycles (IV–VI) are of higher frequency and in phase with the $CaCO_3$ cycles (Fig. 5). *Deflandrea antarctica* also shows this relationship in the same interval (at $CaCO_3$ cycles 6, 7 and 9). Like *V. apertura*, *D. antarctica* is also characteristic for Middle to Late Eocene circum-Antarctic shallow marine conditions (Röhl et al., 2004). Both taxa probably represent heterotrophic dinoflagellates, as suggested by their peridinioid affinity (Sluijs et al., 2005). In addition, relatively high concentrations of representatives of definitively heterotrophic peridinioid genera, such as *Brigantedinium*, *Selenopemphix* and *Lejeunecysta,* are recorded in this interval. All these taxa are characteristic for conditions prevailing in the Ross Sea. The taxa co-occur with high concentrations of diatom tests (Stickley, *unpublished data*). Because diatoms are commonly regarded as a primary food source for heterotrophic dinoflagellates, it may be assumed that in the lower part of the interval conditions (during the Pr2 case) were favourable for specific diatoms that were subsequently grazed upon by the recorded dinoflagellates. Possibly, a reduced sea-ice cover in the Ross Sea enhanced the wind-driven Tasman Current, bringing the Antarctic assemblage to the North. The non-correspondence of $CaCO_3$ and the dinocyst abundance (that shows only minor fluctuations; see Fig. 3) could simply imply that both precession cases were equally productive in terms of cyst production. However, the general inverse correlation of *V. apertura* and the calcium record (see above) suggests that such conditions occurred rarely.

Although some irregularities are observed in the sporomorph record, environmental and climatic conditions on land were probably comparable to those in the upper part of the studied interval (cycles 1–6).

5. Conclusions

The field data presented here clearly show environmental variability on precessional time scales. GCM experiments are used to indicate which mechanisms are most feasible for translating orbital forcing into environmental response. The precession-scale fluctuations in summer precipitation and temperature are the most likely forcings for the identified vegetational changes, here related to variations in the density of *Nothofagus* (*Brassospora*). In the marine realm, the effect of precession forcing is less noticeable, although increased precipitation/runoff seemed to enhance dinoflagellate cyst production variations (Fig. 3). The GCM generates less sea ice in the Ross Sea during Austral summer during Pr2. This is only partly supported by the palynological data (i.e., the influx of Antarctic (proto) peridinioids, such as *V. apertura*, in the lower part of the record).

No evidence is found that precession modulated the surface wind strength driving the Tasman Current, except in Austral winter Pr2 in the Ross Sea area, where wind strength was significantly higher (see Fig. 6 and Table 1). The effect of increased wind, however, was probably small because the sea-ice cover prevented wind–ocean interaction. Lower frequency fluctuations in *V. apertura* indicate that the intensity of the Tasman Current was modulated by fluctuating climate parameters on time scales longer than precession.

The extent of Eocene Antarctic ice sheets is still debated, but some studies agree that small to medium scale mountain glaciation already occurred during the Middle Eocene (Abreu and Anderson, 1998; Zachos et al., 2001; Billups and Schrag, 2003). The present study did not address land ice build up (the GCM had no land-ice model and was run over a time span too short to realistically reflect land-ice dynamics). These lower summer temperatures are further signalled by the reduced amounts of *Nothofagus* (*Brassospora*) pollen. Based on this evidence, we conclude that orbital forcing, and more particularly precessional forcing, may have modulated conditions on Antarctica, and therefore may have played a role in Antarctic glacial dynamics. This conclusion corroborates the concept of DeConto and Pollard (2003b) and DeConto et al. (2007).

Acknowledgements

This research used samples provided by the Ocean Drilling Program (ODP). ODP was sponsored by the U.S. National Science Foundation (NSF) and participating countries under management of Joint Oceanographic Institutions (JOI) Inc. Funding for this research was provided by the Netherlands Council for Earth and Life Sciences (ALW-NWO) to JW and the Deutsche Forschungsgemeinschaft (DFG) to U. Röhl. We are particularly grateful to the lab technicians Natasja Welters and Jan van Tongeren at the Laboratory of palaeobotany and palynology of Utrecht University for their help with processing the palynological samples. We kindly acknowledge John Cann and an anonymous reviewer for the constructive criticism and suggestions.

References

Abreu, V.S., Anderson, J.B., 1998. Glacial eustasy during the Cenozoic: sequence stratigrapic implications. American Association of Petroleum Geologists Bulletin 82, 1385–1400.

Billups, K., Schrag, D.P., 2003. Application of benthic foraminiferal Mg/Ca ratios to questions of Cenozoic climate change. Earth and Planetary Science Letters 209, 181–195.

Brinkhuis, H., Sengers, S., Sluijs, A., Warnaar, J., Williams, G.L., 2003. Latest Cretaceous to earliest Oligocene, and Quaternary dinoflagellates from ODP Site 1172, East Tasman Plateau. In: Exon, N., Kennett, J.P. (Eds.), Proceedings of the Ocean Drilling Program, Scientific Results, volume 189. U.S. Government Printing Office, College Station, Texas.

Burgess, C.E., Pearson, P.N., Lear, C.H., Morgans, H.E.G., Handley, L., Pancost, R.D., Schouten, S., 2008. Middle Eocene climate cyclicity in the southern Pacific: implications for global ice volume. Geology 36, 651–654.

DeConto, R.M., Pollard, D., 2003a. Rapid Cenozoic glaciation of Antarctica induced by declining atmospheric CO_2. Nature 421, 245–249.

DeConto, R.M., Pollard, D., 2003b. A coupled climate-ice sheet modeling approach to the Early Cenozoic history of the Antarctic ice sheet. Palaeogeography, Palaeoclimatology, Palaeoecology 198, 39–52.

DeConto, R., Pollard, D., Harwood, D., 2007. Sea ice feedback and Cenozoic evolution of Antarctic climate and ice sheets. Paleoceanography 22.

Exon, N.J., Kennett, J.P., Malone, M., 2001. Proceedings of the Ocean Drilling Program, Initial Reports, volume 189. U.S. Government Printing Office, College Station, Texas.

Exon, N.F., Kennet, J.P., Malone, M., 2004. Leg 189 synthesis: Cretaceous–Holocene history of the Tasmanian Gateway. In: Exon, N.F., Kennett, J.P., Malone, M.J. (Eds.), Proc. ODP, Sci. Results, 189.

Fensome, R.A., Williams, G.L., 2004. The Lentin and Williams index of fossil dinoflagellates, American Association of Stratigraphic Palynologists Foundation Contr. Series, 2004 edition.

Fuller, M., Touchard, Y., 2004. On the magnetostratigraphy of the East Tasman Plateau, timing of the opening of the Tasmanian Gateway and paleoenvironmental changes. The Cenozoic Southern Ocean. In: Exon, N., Kennett, J.P., Malone, M. (Eds.), Tectonics, sedimentation and climate change between Australia and Antarctica. American Geophysical Union (AGU), Washington, pp. 127–151.

Gradstein, F.M., Ogg, J.G., Smith, A.G., 2004. A geologic timescale 2004. Cambridge University Press, Cambridge. 589 pp.

Hannah, M.J., 1997. Climate controlled dinoflagellate distribution in Late Eocene–earliest Oligocene strata from CIROS-1 drillhole, McMurdo Sound, Antarctica. Terra Antarctica 4, 73–78.

Hay, W.W., DeConto, R., Wold, C.N., Wilson, K.M., Voigt, S., Schulz, M., Wold-Rossby, A., 1999. Alternative global Cretaceous paleogeography, in: the evolution of Cretaceous ocean/climate systems. In: Barrera, E., Johnson, C. (Eds.), Geological Society of America Special Paper, pp. 1–47.

Heiri, O., Lotter, A.F., Lemcke, G., 2001. Loss on ignition as a method for estimating organic and carbonate content in sediments: reproducibility and comparability of results. Journal of Paleolimnology 25, 101–110.

Huber, M., Sloan, L.C., 2000. Climatic responses to tropical sea surface temperature changes on a 'greenhouse' Earth. Paleoceanography 15, 443–450.

Huber, M., Sloan, L.C., 2001. Heat transport, deep waters, and thermal gradients: coupled simulation of an Eocene 'Greenhouse' climate. Geophysical Research Letters 28, 3481–3484.

Huber, M., Nof, D., 2006. The ocean circulation in the southern hemisphere and its climatic impacts in the Eocene. Palaeogeography, Palaeoclimatology, Palaeoecology 231, 9–28.

Huber, M., Brinkhuis, H., Stickley, C.E., Doos, K., Sluijs, A., Warnaar, J., Schellenberg, S.A., Williams, G.L., 2004. Eocene circulation of the Southern Ocean: was Antarctica kept warm by subtropical waters? Paleoceanography 19 (4026), 4021-4012.

Kerr, A., Huybrechts, P., 1999. The response of the East Antarctic ice-sheet to the evolving tectonic configuration of the Transantarctic Mountains. Global and Planetary Change 23, 213–229.

Kürschner, W.M., Wagner, F., Dilcher, D.L., Visscher, H., 2001. Using fossil leaves for the reconstruction of Cenozoic paleoatmospheric CO_2 concentrations. In: Gerard, L.C., Harrisson, W.E., Hanson, B.M. (Eds.), Geological perspectives of global climate change. The American Association of Petroleum Geologists (AAPG), Tulsa, pp. 169–189.

Langford, R.P., Wilford, G.E., Truswell, E.M., Isern, A.R., 1995. Palaeogeographic atlas of Australia. Volume 10 — Cainozoic. Australian Geological Survey Organization, Canberra. 38 pp.

Macphail, M.K., Truswell, E.M., 2004. Palynology of Site 1166, Prydz Bay, East Antarctica. In: O'Brien, P.E., Cooper, A.K., Richter, C. (Eds.), Proceedings of the Ocean Drilling Program, Scientific Results, vol. 188. U.S. Government Printing Office, College Station, Texas.

Mildenhall, D.C., Hollis, C.J., Naish, T.R., 2004. Orbitally-influenced vegetation record of the Mid-Pleistocene Climate Transition, onshore eastern New Zealand (ODP Leg 181, Site 1123). Marine Geology 205, 87–111.

Mohr, B.A.R., 1990. Eocene and Oligocene sporomorphs and dinoflagellate cysts from leg 113 drill sites, Weddel Sea, Antarctica. In: Barker, P.F., Kennet, J.P. (Eds.), Proceedings of the Ocean Drilling Program, Scientific Results, vol. 113. U.S. Government Printing Office, College Station, Texas, pp. 595–611.

Norvick, M.S., Smith, M.A., 2001. Mapping the plate tectonic reconstruction of southern and southeastern Australia and implications for petroleum systems. APPEA Journal 41, 15–36.

Pagani, M., Zachos, J.C., Freeman, K.H., Tipple, B., Bohaty, S., 2005. Marked decline in atmospheric carbon dioxide concentrations during the Paleogene. Science 309, 600–603.

Pearson, P.N., Palmer, M.R., 2000. Atmospheric carbon dioxide concentrations over the past 60 million years. Nature 406, 695–699.

Quilty, P.G., 1997. Eocene and younger biostratigraphy and lithofacies of the Cascade Seamount, East Tasman Plateau, southwest Pacific Ocean. Autralian Journal of Earth Sciences 44, 655–665.

Reichart, G.-J., Brinkhuis, H., 2003. Late Quaternary Protoperidinium cysts as indicators of paleoproductivity in the northern Arabian Sea. Marine Micropaleontology 49, 303–315.

Robert, C., 2004. Cenozoic environments in the Tasmanian area of the Southern Ocean (ODP Leg 189): inferences from bulk and clay mineralogy. Geophysical Monograph Series 151, 127–151.

Röhl, U., Brinkhuis, H., Stickley, C.E., Fuller, M., Schellenberg, S.A., Wefer, G., Williams, G.L., 2004. Sea level and astronomically induced environmental changes in Middle and Late Eocene sediments from the East Tasman Plateau. In: Exon, N.F., Malone, M., Kennett, J.P. (Eds.), Climate Evolution in the Southern Ocean and Australia's Cenozoic flight northward from Antarctica. American Geophysical Union, Geophysical Monograph Series, 151, 127–151.

Roth-Nebelsick, A., Utescher, T., Mosbrugger, V., Diester-Haass, L., Walther, H., 2004. Changes in atmospheric CO_2 concentrations and climate from the Late Eocene to Early Miocene: palaeobotanical reconstruction based on fossil floras from Saxony, Germany. Palaeogeography, Palaeoclimatology, Palaeoecology 205, 43–67.

Royer, J.Y., Rollet, N., 1997. Plate-tectonic setting of the Tasman region. Australian Journal of Earth Sciences 44, 543–560.

Ruddiman, W.F., 2001. Earth's climate, past and future. W. H., Freeman and Company.

Sloan, L.C., Rea, D.K., 1995. Atmospheric carbon dioxide and Early Eocene climate: a general circulation modeling sensitivity study. Palaeogeography, Palaeoclimatology, Palaeoecology 119, 275–292.

Sloan, L.C., Morrill, C., 1998. Orbital forcing and Eocene continental temperatures. Palaeogeography, Palaeoclimatology, Palaeoecology 144, 21–35.

Sloan, L.C., Huber, M., 2001. Eocene oceanic responses to orbital forcing on precessional time scales. Paleoceanography 16, 101–111.

Sluijs, A., Pröss, J., Brinkhuis, H., 2005. From greenhouse to icehouse; organic walled dinoflagellate cysts as paleoenvironmental indicators in the Paleogene. Earth-Science Reviews 68, 281–315.

Sluiter, I.R.K., Kershaw, A.P., Holdgate, G.R., Bulman, D., 1995. Biogeographic, ecological and stratigraphic relationships of the Miocene brwon coal floras, Latrobe Valley, Victoria, Australia. International Journal of Coal Geology 28, 277–302.

Warnaar, J., 2006. Climatological implications of Australian–Antarctic separation: LPP Contributions series no. 22. Utrecht.

Wasmund, N., Zalewski, M., Busch, S., 1999. Phytoplankton in larger river plumes in the Baltic Sea. ICES Journal of Marine Science 56, 23–32.

Williams, G.L., Brinkhuis, H., Pearce, M.A., Fensome, R.A., Weegink, J.W., 2004. Southern Ocean and global dinoflagellate cyst events compared: index events for the Late Cretaceous–Neogene. Proceedings of the Ocean Drilling Program: In: Exon, N.F., Kennett, J.P., Malone, M.J. (Eds.), Scientific Results, vol. 189, pp. 1–98. 189.

Wilson, G.J., 1967. Some new species of Lower Tertiary dinoflagellates from McMurdo Sound. Antarctica, New Zealand Journal of Botany 5, 57–83.

Zachos, J., Pagani, M., Sloan, L., Thomas, E., Billups, K., 2001. Trends, rythms, and aberrations in global climate 65 Ma to present. Science 292, 686–693.